

UC San Diego

UC San Diego Electronic Theses and Dissertations

Title

The Role of Alpha Protein Kinase 3 in Cardiac Development and Function

Permalink

<https://escholarship.org/uc/item/7bj958tm>

Author

Wang, Li

Publication Date

2021

Peer reviewed|Thesis/dissertation

UNIVERSITY OF CALIFORNIA SAN DIEGO

The Role of Alpha Protein Kinase 3 in Cardiac Development and Function

A thesis submitted in partial satisfaction of the requirements
for the degree Master of Science

in

Biology

by

Li Wang

Committee in Charge:

Professor Ju Chen, Chair
Professor Amy Pasquinelli, Co-chair
Professor Deborah Yelon

2021

The thesis of Li Wang is approved, and it is acceptable in quality and form for publication on microfilm and electronically.

University of California San Diego

2021

DEDICATION

To mom and dad, who enable me to pursue my dream through their unconditional love and tremendous sacrifice.

To my roommates, Shelveen, Gary, and Luis, who have always stood by my side through the ups and downs of my undergraduate years and beyond.

To my friends, who have been supportive in my life and made me grow as a person.

TABLE OF CONTENTS

| | |
|------------------------------|------|
| Thesis Approval Page..... | iii |
| Dedication..... | iv |
| Table of Contents | v |
| List of Figures | vi |
| List of Tables | vii |
| Acknowledgement | viii |
| Abstract of the Thesis | x |
| Introduction | 1 |
| Methods and Materials | 5 |
| Results..... | 11 |
| Discussion | 28 |
| Appendix..... | 33 |
| References | 36 |

LIST OF FIGURES

| | |
|---------------|----|
| Figure 1..... | 12 |
| Figure 2..... | 16 |
| Figure 3..... | 19 |
| Figure 4..... | 22 |
| Figure 5..... | 27 |

LIST OF TABLES

Table 1 25

ACKNOWLEDGEMENTS

I would like to acknowledge Prof. Ju Chen for the privilege to be a member in his cardiology research laboratory. The past four years in his lab has truly been the highlight in my education at UCSD. Ju has always been a supportive mentor, both in my academic career and my personal development. The guidance and learning opportunities I have received from him in the early stages of my academic career served as a catalyst in my pursuit of research. I would also like to acknowledge Dr. Wei Feng for his continuous and delicate mentoring in the lab. From using a micropipette to performing immunofluorescent microscopic analysis, the techniques I learned from Wei brought me into the world of experimental science. My day-to-day research would not have been possible without his tireless mentoring. I also sincerely appreciate the feedbacks I received on my thesis writing from Ju and Wei.

Additionally, I would like to acknowledge Prof. Amy Pasquinelli for being an exceptional educator. Her lectures provided me with a solid foundation in molecular biology, which enabled me to investigate the molecular mechanisms underlying human diseases. I also greatly appreciate the time from Prof. Amy Pasquinelli and Prof. Deborah Yelon spent for serving on my thesis committee.

Last but not least, I would like to thank the project scientists, postdoctoral scholars, and graduate students in our lab for their support as well as insightful discussions on my research project. Through them, I learned the rigor and commitment necessary in scientific research. Each of them contributed an invaluable part to my growth as a scientific researcher, which I am forever grateful for.

In this thesis, the mouse models generated by CRISPR-Cas9 genome editing technology were designed by Dr. Wei Feng. The delivery of CRISPR-Cas9 components by microinjection was performed by the Transgenic Core at UCSD School of Medicine. Echocardiography was performed by the Seaweed lab at UCSD School of Medicine. Mass

spectrometry was performed by the Proteomics Shared Resource at Sanford Burnham Prebys Medical Discovery Institute.

ABSTRACT OF THE THESIS

The Role of Alpha Protein Kinase 3 in Cardiac Development and Function

by

Li Wang

Master of Science in Biology

University of California San Diego, 2021

Professor Ju Chen, Chair
Professor Amy Pasquinelli, Co-chair

Alpha Protein Kinase 3 (ALPK3) is an alpha kinase highly expressed in skeletal and cardiac muscles. Recent studies reveal that the biallelic truncating mutations in ALPK3 are associated with pediatric cardiomyopathy in human patients, suggesting that ALPK3 plays an essential role in cardiac development and function. However, no *in vivo* studies have elucidated

the cardiac function of ALPK3; the subcellular localization of ALPK3 in cardiomyocyte is unknown, and whether the putative kinase activity is essential for the function of ALPK3 remains to be investigated. Utilizing ALPK3 global and cardiac specific knock out mouse models, we show that both the global and cardiac specific loss of ALPK3 leads to progressive dilated cardiomyopathy and premature lethality in mice. To investigate whether the putative kinase activity of ALPK3 is essential for its cardiac function, we mutate the invariant catalytic lysine residue in the alpha kinase domain of ALPK3 in mice and show that mice harboring the homozygous lysine mutation do not develop cardiac defects. Our *in vitro* and *in vivo* data further indicate that ALPK3 localizes in the nucleus of cardiomyocyte. In summary, our present study suggests that ALPK3 is a nucleus-localized protein indispensable for cardiac development and function, and that ALPK3 functions by protein-protein interactions independently of its putative kinase activity in heart.

INTRODUCTION

Heart disease is the number one cause of death in the United States (Kochanek *et al.*, 2020). The economic burden of heart disease, including direct medical expenses and indirect loss in productivity, was 219.6 billion dollars in the United States in 2017, making heart disease the fourth most costly medical condition (Virani *et al.*, 2021). Cardiomyopathies are a group of heart diseases in which myocardium exhibits mechanical and/or electrical dysfunction (Maron *et al.*, 2006). Cardiomyopathies are frequently caused by genetic factors and usually have the structural representations of inappropriate ventricular hypertrophy or dilation (Maron *et al.*, 2006). In hypertrophic cardiomyopathy (HCM), left ventricle becomes hypertrophic in the absence of another cardiac disease or systemic condition that could account for the degree of hypertrophy (Goldman and Schafer, 2015). In dilated cardiomyopathy (DCM), the left ventricle or both ventricles exhibits enlargement and systolic dysfunction in the absence of coronary artery disease, valvular abnormalities, or pericardial disease (Goldman and Schafer, 2015). DCM is usually irreversible and the most common cause of heart failure (Maron *et al.*, 2006). In addition to the adult population, DCM is also the most common form of cardiomyopathy diagnosed in children, accounting for up to 58% of the pediatric cardiomyopathy cases (Braunwald and Marian, 2017; Maron *et al.*, 2006). Pediatric cardiomyopathy frequently necessitates heart transplant in children (Braunwald and Marian, 2017; Brieler *et al.*, 2017), which is challenging due to an increasing number on the waitlist for heart transplant (Braunwald and Marian, 2017). Thus, understanding the mechanisms underlying pediatric DCM is imperative for developing effective therapeutics to alleviate its associated mortality.

Physiological homeostasis is regulated by a variety of mechanisms, a major one of which is the reversible phosphorylation by kinases and dephosphorylation by phosphatases of proteins (Middelbeek *et al.*, 2010). Protein kinases function either via their phospho-transferase activity, or by interacting with different protein partners in the case of pseudokinases, which lack phospho-transferase activity (Boudeau *et al.*, 2006). Based on the amino acid sequence

similarity in their catalytic core domains, protein kinases can be classified into conventional protein kinases (CPKs), which share similar sequences in their catalytic domain and are identified first historically, and atypical protein kinases (APKs), which do not share the same catalytic core sequence as CPKs and are discovered later (Middelbeek *et al.*, 2010). Despite their little sequence similarity, APKs resemble some of the characteristic secondary protein structures in the catalytic core of CPKs (Middelbeek *et al.*, 2010; Scheeff, Eric D. and Bourne, Philip E, 2005). Nonetheless, since APKs are presented alongside with CPKs in prokaryotes and eukaryotes, it has been proposed that APKs play a unique regulatory role in cells instead of simply being a duplication of CPKs (Middelbeek *et al.*, 2010). The roles of APKs are further implicated by their associations with human diseases, such as Atypical Protein Kinase C (aPKC) in neurodegenerative disease (Shao *et al.*, 2006), Eukaryotic Elongation Factor 2 Kinase (eEF2K) in lung cancer (Bircan *et al.*, 2018), and recently, Alpha Protein Kinase 3 (ALPK3) in heart disease (Almomani *et al.*, 2016). The associations between APKs and human diseases suggest that APKs are indispensable for physiological homeostasis.

While the APK superfamily is present in both prokaryotes and eukaryotes, the alpha protein kinase family, a unique sub-family of APKs distinguished by their shared alpha kinase domain, is only present in eukaryotes, including vertebrates and invertebrates (Middelbeek *et al.*, 2010). Hence, alpha kinases have been suggested to provide a novel regulatory mechanism in complex eukaryotic organisms (Middelbeek *et al.*, 2010; Scheeff, Eric D. and Bourne, Philip E, 2005). In human, six alpha kinases have been identified, including Eukaryotic Elongation Factor 2 Kinase (eEF2K), Transient Receptor Potential cation channel subfamily M member 6 (TRPM6), Transient Receptor Potential cation channel subfamily M member 7 (TRPM7), Alpha Protein Kinase 1 (ALPK1), or lymphocyte alpha protein kinase, Alpha Protein Kinase 2 (ALPK2), or heart alpha protein kinase, and Alpha Protein Kinase 3 (ALPK3), or muscle alpha protein kinase (Middelbeek *et al.*, 2010). Alpha protein kinases play diverse cellular and physiological roles, including regulation on global protein synthesis by eEF2K (Horman *et al.*, 2002), ion

transport and homeostasis by TRPM6 and TRPM7 (Schlingmann *et al.*, 2007), and innate immune response by ALPK1 (Zhou *et al.*, 2018). The diverse functions of alpha kinases implicate their regulatory roles in higher vertebrate organisms and in human health.

Among the six alpha kinases in human, ALPK2 and ALPK3 have their highest expressions in heart (Fagerberg *et al.*, 2014), yet the functional studies on them have been limited. Our previous study revealed that mice with global loss of ALPK2 developed normally and did not have cardiac defects, suggesting that ALPK2 is dispensable for cardiac function under normal physiological condition (i.e. without challenges such as pressure overload in heart) (Bogomolovas *et al.*, 2020); no genetic mutations in ALPK2 have been reported to be associated with heart diseases in human either. Interestingly, ALPK3, which shares structural similarities with ALPK2 (Middelbeek *et al.*, 2010), has recently been reported to be associated with pediatric cardiomyopathy extensively. Biallelic truncating mutations in ALPK3 have been identified as the genetic causes of various cases of pediatric dilated cardiomyopathy; most of those patients developed DCM and either died in their childhood or underwent heart transplants (Almomani *et al.*, 2016; Çağlayan *et al.*, 2017; Herkert *et al.*, 2020; Jaouadi *et al.*, 2018). Due to the implication of ALPK3 in pediatric cardiomyopathy, investigating the cardiac specific function of ALPK3 is significant to the development of therapeutic treatments for ALPK3 associated pediatric cardiomyopathy and will provide mechanistic insights into cardiomyopathy in general. A previous study suggests that ALPK3 localizes in the nucleus of COS cell, a transformed monkey epithelial cell line (Gluzman, 1981), and that ALPK3 might play a role in gene regulation (Hosoda *et al.*, 2001). However, whether ALPK3 localizes in the nucleus of cardiomyocyte remains to be verified, and the potential genes whose expressions are regulated by ALPK3 in cardiomyocyte have yet to be identified. Additionally, while ALPK3 contains an alpha kinase domain at its extreme C terminal (Middelbeek *et al.*, 2010), whether ALPK3 functions via its putative kinase activity is unknown.

Using genetically engineered mouse models along with physiological, biochemical, and molecular biology approaches, our present study aims to investigate the *in vivo* role of ALPK3 in cardiac development and function. Our data suggest that ALPK3 is a nucleus-localized protein essential for cardiac development and function, and that the global and cardiac specific loss of ALPK3 leads to progressive dilated cardiomyopathy. Our study further suggests that ALPK3 functions by interacting with proteins essential for cardiac function, independently of its putative kinase activity in its alpha kinase domain.

METHODS AND MATERIALS

Animal study approval

All animal studies were performed in accordance with the *Guide for the Care and Use of Laboratory Animals*, published by the National Academies Press (US), 2011, 8th Edition, and according to protocols approved by the Institutional Animal Care and Use Committee at the University of California San Diego.

Mice

Mice with *Alpk3* exon 3 flanked by LoxP sites (EMMA:09571) were purchased from the International Knockout Mouse Consortium. Those mice were then crossed with flippase deleter mice (Rodríguez *et al.*, 2000) to remove the LacZ and Neo cassettes. To generate ALPK3 global knock out (gKO) mice, *Alpk3* exon 3^{flxed/flxed} (*Alpk3^{ff}*) mice were first crossed with Sox2-Cre global deleter mice (Hayashi *et al.*, 2002) to generate ALPK3 heterozygous mice (+/-). Heterozygous mice were further subjected to crossbreeding to generate -/- (gKO) mice or +/- control littermates (Ctrl) (Figure 1a). To generate ALPK3 cardiac specific conditional knock out (cKO) mice, *Alpk3^{ff}* mice were first crossed with α MHC-Cre transgenic mice (Agah *et al.*, 1997) to generate *Alpk3^{ff/+}; α MHC-Cre* mice. *Alpk3^{ff/+}; α MHC-Cre* mice were further crossed with *Alpk3^{ff}* mice to generate *Alpk3^{ff}; α MHC-Cre* (cKO) or *Alpk3^{ff}* control littermates (Ctrl). Genotypes of gKO mice were analyzed by polymerase chain reaction (PCR) with a pair of KO allele specific primers and a pair of wildtype specific primer. cKO mice were analyzed PCR using a pair of LoxP primers and a pair of α MHC-Cre primers. ALPK3 lysine 1420 to arginine (K1420R) mutation knock in mice were generated by CRISPR-Cas9 genome editing system (Figure 3b). Cas9 enzyme, crRNA, tracrRNA, and an HDR template carrying an AGG codon encoding for arginine at ALPK3 p.1420 position were mixed and then microinjected into the pronuclei of mouse zygotes at UCSD Transgenic Core. The zygotes were then inoculated in a

surrogate mouse. K1420R knock in mouse founders were validated by PCR analysis using a pair of mutation specific primers and by sequencing. Male K1420R knock-in mice were bred with female C57B/6 mice to generate germline-transmittable K1420R knock in mice. ALPK3-3xFLAG knock-in mice were generated similarly by CRISPR-Cas9 genome editing system, with an HDR template carrying a 3xFLAG cassette.

Echocardiography

The detailed protocol was described in the lab's previous publication (Liu *et al.*, 2019). Briefly, mice were anesthetized with 5% isoflurane for 15 seconds and maintained at 0.5% isoflurane for the duration of the study. Echocardiography was performed by VisualSonics, SonoSite FUJIFILM, Vevo 2100 ultrasound system with a linear transducer 32-55MHz. Left ventricle internal dimension at end-diastole (LVIDd) and left ventricle internal dimension at end-systole (LVIDs) were measured using M-mode tracing. Fraction shortening (FS) or ejection fraction (EF) measurements were used as an indicator for cardiac contractile function.

Western blotting

Western blotting was performed as described in the lab's previous publications (Mu *et al.*, 2020) with modifications. For tissue protein extraction, mice were first sacrificed, and their tissues were harvested. The tissues were lysed in ice cold RIPA buffer (25 mM Tris•HCl pH 7.6, 150 mM sodium chloride, 1% NP-40, 1% sodium deoxycholate, 0.1% sodium dodecyl sulfate) with a protease inhibitor cocktail (cOmplete™, Millipore Sigma). For protein extraction from cells, 100µL of ice cold RIPA buffer was added to each 35mm cell culture dish. Cells were incubated with RIPA buffer on ice for 5 min, and the protein lysate was collected and transferred to a 1.7mL Eppendorf tube. The protein concentration of the lysates was measured using a BCA protein quantification assay (Pierce™, Thermo Fisher) for loading adjustment. LDS sample buffer (NuPAGE™, Thermo Fisher) was added to protein lysates, and the lysates were

subjected to SDS-PAGE electrophoresis using 4-12% Bis-Tris gels (Bolt™, Thermo Fisher) in MOPS-SDS or MES-SDS running buffer according to the manufacturer's recommended protocols and then transferred to a PVDF membrane at 4°C overnight with 30V direct current. The blots were then blocked in PBS with 5% dry milk at room temperature for 1 hour and incubated with primary antibodies at 4°C overnight. The blots were washed with PBS with 0.1% Triton X-100 (PBST) and incubated with HRP-conjugated secondary antibodies at room temperature for 1 hour. After a final wash with PBST, proteins of interest were visualized by the addition of Clarity Western ECL Substrate™ (Bio-Rad). Image capture was performed using a ChemiDoc™ Imaging System (Bio-Rad).

Histology

Histology study was performed as described previously (Mu *et al.*, 2020). Briefly, mouse hearts were dissected out at indicated stages, fixed in 4% paraformaldehyde in PBS, and dehydrated through 50%-100% ethanol. The mouse hearts were then embedded in paraffin and cut into 8µm thin sections by a microtome. Slides were then stained by Hematoxylin & Eosin stain and scanned by a NanoZoomer 2.0HT Slide Scanning System (Hamamatsu).

Quantitative real time polymerase chain reaction (qRT-PCR)

qRT-PCR analysis was performed according to the lab's previous publications (Fang *et al.*, 2017; Wu *et al.*, 2017) with modifications. Briefly, total RNA from tissues was isolated using TRIzol™ reagent (Invitrogen™, Thermo Fisher) according to the manufacturer's recommended protocol. The concentration of RNA was measured using a NanoDrop™ 2000 spectrophotometer (Thermo Fisher). cDNA was then synthesized from 2 µg total RNA using a High Capacity cDNA Reverse Transcription Kit. Real-time PCR was performed with iTaq™ Universal SYBR® Green Supermix (Bio-Rad) using an iCycler real-time PCR detection system

(IQ5, Bio-Rad). Gene expression was represented as the ΔC_T value normalized to the reference gene Gapdh. The $\Delta\Delta C_T$ value for each target gene was then calculated by subtracting the average ΔC_T from the control group. Finally, the n-fold difference was calculated using $2^{-\Delta\Delta C_T}$ method. Data were collected and analyzed in triplicate.

In silico prediction of nuclear localization signals

In silico prediction of ALPK3 nuclear localization signals was performed on SeqNLS web interface (<http://mleg.cse.sc.edu/seqNLS/>) using the default parameters.

GFP-ALPK3 plasmid construction

The strategy of molecular cloning and mutagenesis was described previously (Liu *et al.*, 2019). The cDNA of mouse APLK3 (Cat: MR218500) was purchased from Origene (Rockville, MD). cDNA of ALPK3 full-length and truncations were produced by PCR and cloned into pCMV6-AN-mGFP (Origene) for mammalian expression studies.

Cell culture and transfection

H9C2 cells were plated on a 10cm tissue culture dish coated with 0.2% gelatin. Cells were cultured by Dulbecco's Modified Eagle Medium (DMEM) with 10% fetal bovine serum (FBS) at 37°C with 5% CO₂. Cells were passaged and seeded on a 35mm confocal dish coated with 0.2% gelatin at 50% confluence before transfection. Transfection was performed with a Lipofectamine™ 3000 kit (Thermo Fisher) according to the manufacturer's recommendation. Briefly, 1µg of plasmid was mixed with Lipofectamine™ 3000 transfection reagent, incubated at room temperature for 15 min, and added to the cells in 35mm confocal dish. Cells were incubated at 37°C with 5% CO₂ for 24 hrs before imaging.

Fluorescent microscopy

Fluorescent microscopic images were acquired by an Echo Revolve microscope.

FLAG co-immunoprecipitation (co-IP)

30mg of cardiac tissue was lysed in RIPA buffer (25 mM Tris•HCl pH 7.6, 150 mM sodium chloride, 1% NP-40, 1% sodium deoxycholate, 0.1% sodium dodecyl sulfate) with a 1mg tissue to 20 μ L ratio. The lysate was cleared by centrifugation, and the supernatant was incubated with anti-FLAG[®] M2 beads (Sigma) for 1hr at 4°C. After 1hr, the beads were washed with RIPA buffer for 5 min x 3 times at 4°C. After washing, the beads were proceeded to mass spectrometry for the identification of precipitated peptides, or the beads-bound peptides were eluted by 2X Laemmli buffer (Bio-Rad) by boiling at 70°C for 3 min for downstream Western blot analysis.

Mass spectrometry and statistical filtering

Mass spectrometry was used to identify the immunoprecipitated peptides from FLAG co-IP. To be considered as significantly enriched, a specific peptide needed to be present or absent in both homozygous ALPK3-3xFLAG samples, with a fold enrichment in ALPK3-3xFLAG samples above 2. Mass spectrometry was performed by Sanford Burnham Prebys Proteomics Shared Resource.

Gene ontology analysis

Gene ontology analysis on biological function was performed on the Gene Ontology Resource web interface (<http://geneontology.org>). Parameters: analysis type = PANTHER Overrepresentation Test (Released 20200728), GO database DOI = 10.5281/zenodo.4081749

(release: 2020-10-09), reference list = *Mus musculus*, test type = FISHER, correction = FDR.

Cardiac tissue subcellular fractionation

Tissue subcellular fraction was performed using a Subcellular Protein Fractionation Kit for Tissues (Thermo fisher) according to the manufacturer's protocol. Briefly, 50mg to 100mg of mouse heart tissue was homogenized by cytoplasmic extraction buffer (CEB) for the extraction of cytoplasmic proteins. The remaining pellet portion after CEB extraction was subsequently extracted by membrane extraction buffer (MEB), nuclear extraction buffer (NEB), micrococcal nuclease, and pellet extraction buffer (PEP) for the selective extractions of membrane bound proteins, nuclear proteins, chromatin bound proteins, and cytoskeletal proteins. Each extract was then analyzed by western blot.

Statistical analysis

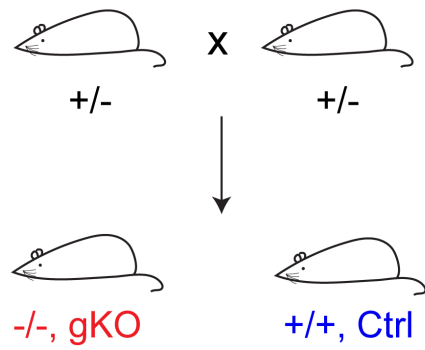
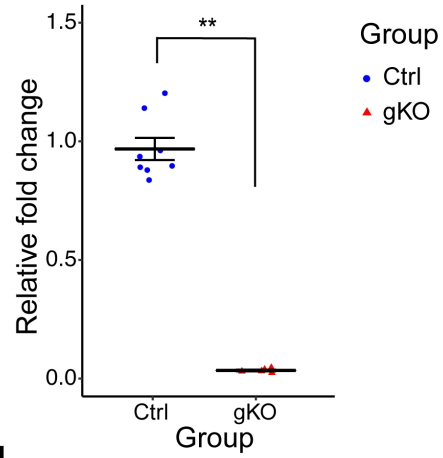
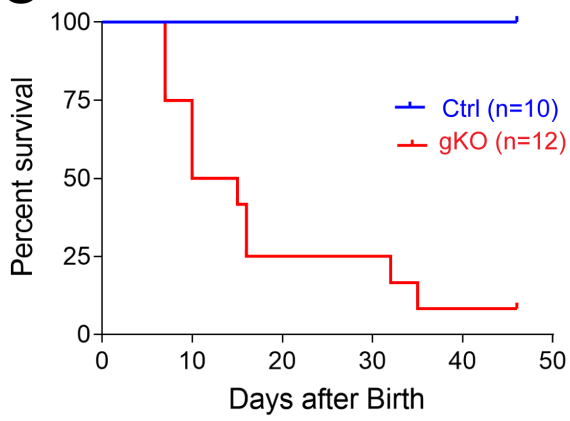
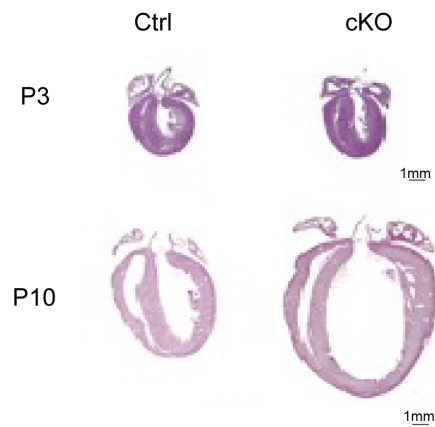
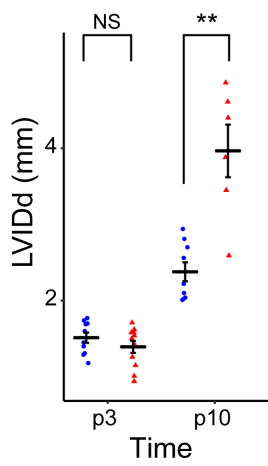
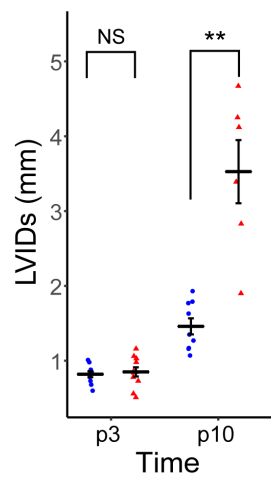
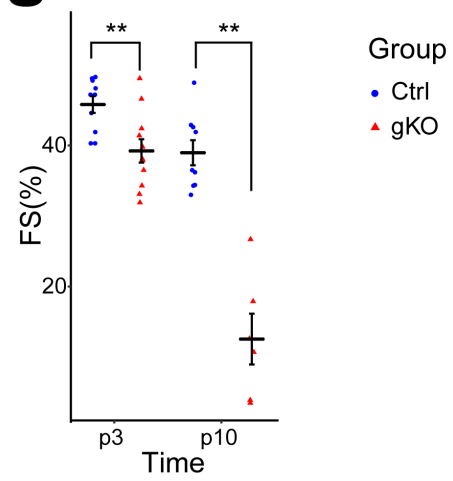
Power analysis software suite G*Power was used to estimate the minimum number of biological replicates required to achieve a statistical power of >0.8 at alpha <0.05. Unless indicated otherwise, all data from the project were analyzed by Student's t-test or analysis of variance followed by Tuckey's post-hoc test for multiple comparisons using Graphpad Prism 8 software (San Diego, CA) or R (www.r-project.org). Differences were significant when $p < 0.05$. Statistical data visualization and graphing were performed using Graphpad Prism 8 or R.

RESULTS

ALPK3 global knockout mice exhibited premature lethality and dilated cardiomyopathy

To investigate whether the global ablation of ALPK3 resembled the cardiac defects observed in human patients with biallelic truncating mutations in ALPK3, we first generated ALPK3 global knockout mice (gKO) by crossing ALPK3 floxed mice with Sox2-Cre global deleter mice (Hayashi *et al.*, 2002) (Method—Mice & Figure 1a). Since no available antibodies were able to detect the endogenous ALPK3 protein in mice, qRT-PCR analysis was performed on the total RNA extracted from gKO mice and their control littermates to assess their mRNA levels of *Alpk3*. gKO hearts had a 90% reduction in *Alpk3* mRNA level compared to Ctrl hearts, indicating the efficient ablation of ALPK3 expression in gKO mouse hearts (Figure 1b). Kaplan-Meier survival analysis showed that 50% of gKO mice died within 10 days after birth, and 75% of gKO mice died within 1 month after birth (Figure 1c), indicating that gKO mice exhibited premature lethality. To characterize the cardiac phenotypes of gKO mice, we performed histology studies and echocardiographic studies at postnatal day 3 (P3) and postnatal day 10 (P10), a period corresponding to the steepest drop in gKO mouse survival (Figure 1c). The histology studies revealed that gKO hearts had a comparable morphology to Ctrl hearts at P3 but a markedly enlarged left ventricle at P10 (Figure 1d). Echocardiographic studies further showed that gKO mice had a significantly increased left ventricular size, as indicated by their increased left ventricle internal dimensions at end diastole (LVIDd) and at end systole (LVIDs) (Figure 1e-f), as well as a significantly decreased cardiac contractile function, as indicated by their percent fraction shortening (FS), at P10 (Figure 1g). Together, those data indicated that global loss of ALPK3 led to early onset and progressive dilated cardiomyopathy in mice, and that ALPK3 gKO mice recapitulated the DCM symptoms in human patients with ALPK3 biallelic truncating mutations.

Figure 1. Global loss of ALPK3 led to premature lethality and dilated cardiomyopathy in mice. **(a)** Strategy for generating ALPK3 global knockout (gKO) mice. ALPK3 floxed mice were first crossed with global deleter Sox2-Cre mice to generate ALPK3 heterozygous mice (+/-). ALPK3 heterozygous mice were then inter crossed, generating ALPK3 global knock out (-/-, gKO) and control littermates (+/+, Ctrl). **(b)** qRT-PCR measurement of Alpk3 mRNA levels in Ctrl (n=8) and gKO (n=5) mouse hearts. mRNA levels were normalized to Gapdh. **, $p < 0.01$ by Student's t-test. **(c)** Kaplan-Meier survival analysis of Ctrl and ALPK3 gKO mice. **(d)** H&E staining of Ctrl and ALPK3 gKO heart sections at postnatal day 3 (P3) and postnatal day 10 (P10). Scale bar, 1mm. **(e)-(g)** Echocardiography measurements of left ventricular internal diameter at **(e)** end-diastole (LVIDd), **(f)** end-systole (LVIDs), and **(g)** left ventricular (LV) systolic function (% of fractional shortening, FS) in Ctrl (blue, n=10) and gKO (red, n=5-10) mice at P3 and P10 time points. NS, not statistically significant; **, $p < 0.01$ by Student's t-test.

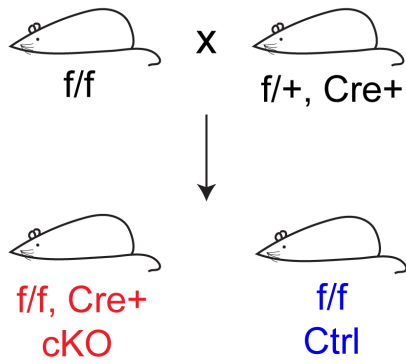
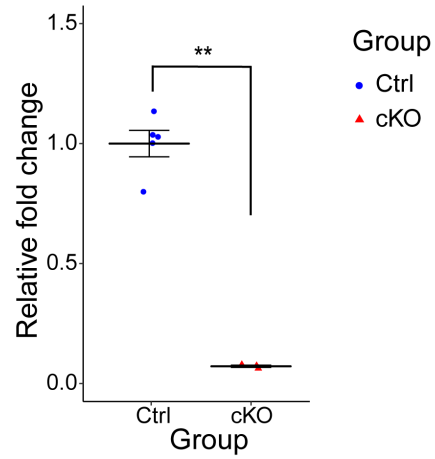
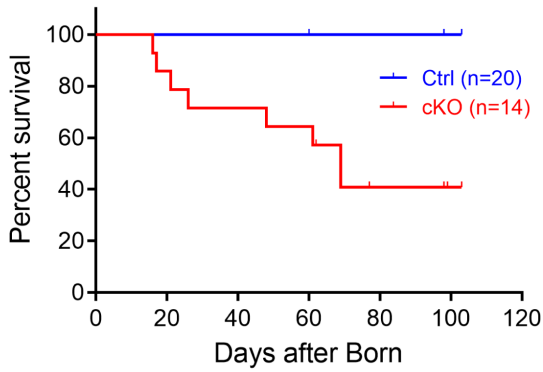
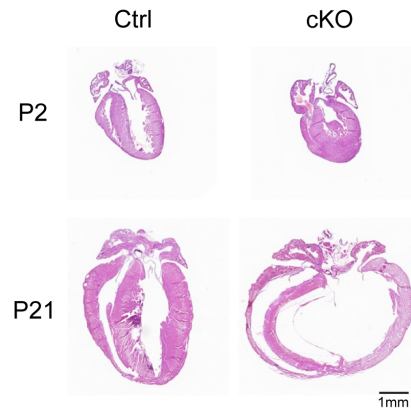
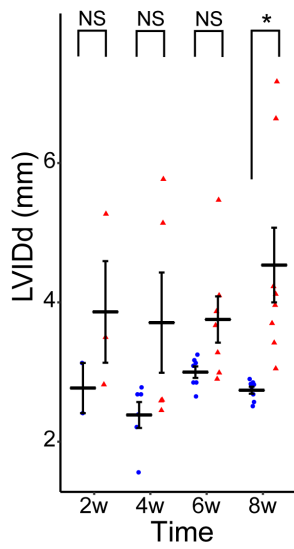
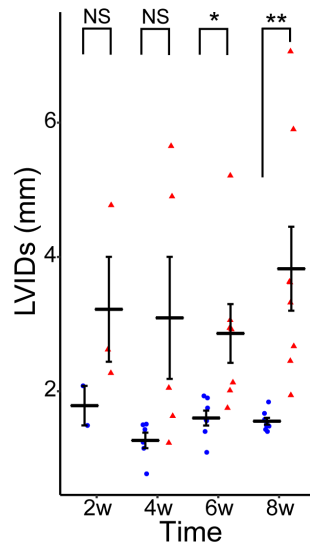
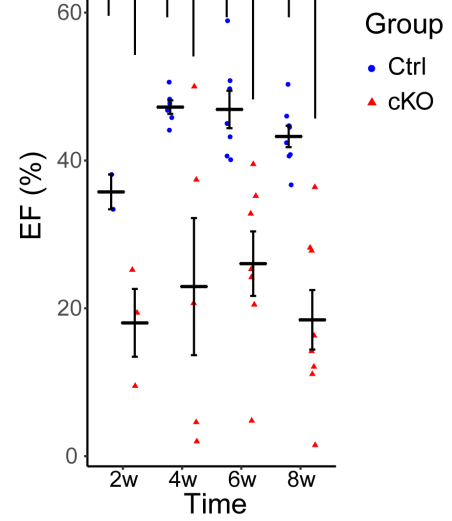
a**b****c****d****e****f****g**

Cardiac specific loss of ALPK3 led to dilated cardiomyopathy in mice

To exclude the possibility that the DCM phenotypes observed in ALPK3 gKO mice were a secondary effect of the loss of ALPK3 in non-cardiac tissues, we next crossed ALPK3 floxed mice with α MHC-Cre transgenic mice (Agah *et al.*, 1997), which have Cre recombinase specifically expressed in cardiac tissue, to generate ALPK3 cardiac specific conditional knockout (Alpk3^{fl/fl}; α MHC-Cre+, cKO) mice (Method—Mice & Figure 2a). qRT-PCR analysis revealed that cKO hearts had a near 90% reduction in Alpk3 mRNA level compared to the control hearts (Alpk3^{fl/fl}, Ctrl) (Figure 2b), indicating the successful ablation of ALPK3 expression in cKO hearts. Consistent with the observations in ALPK3 gKO mice, cKO mice exhibited premature lethality. cKO mice started to die at postnatal day 18 (P18), and about 50% cKO mice died within 2 months after birth (Figure 2c). To examine whether cKO mice exhibited cardiac defects, we performed histology studies to assess their cardiac morphology at postnatal day 2 (P2), a time point just after birth, and postnatal day 21 (P21), a time point at which cKO just started to die. Similar to the observations in gKO mice, cKO mice had a markedly enlarged left ventricle at P21 but a normal left ventricle morphology at P2 (Figure 2d). To further assess the heart dimension and function of cKO mice quantitatively, we performed echocardiographic studies at 2-week, 4-week, 6-week, and 8-week of age, a period corresponding to the steepest decrease in cKO survival rate (Figure 2c). The left ventricular dimension gradually increased from 2-week to 8-week and became significantly different from Ctrl mice in LVIDd at 8-week timepoint (Figure 2e) and in LVIDs at 6-week timepoint (Figure 2f). The contractile function, as indicated by % ejection fraction (ES), started to decrease significantly from 2-week timepoint and continued decreasing till 8-week timepoint (Figure 2g). Hence, the cardiac specific loss of ALPK3 led to DCM in mice, and the DCM phenotypes observed in gKO mice were not merely a secondary consequence to the loss of ALPK3 in non-cardiac tissues. The cardiac phenotypes from ALPK3 gKO and cKO mice indicated that ALPK3 had a specific role in cardiac

development and function. Those data prompted us to investigate the mechanism by which ALPK3 exerted its cardiac specific function.

Figure 2. Cardiac specific loss of ALPK3 led to premature lethality and dilated cardiomyopathy in mice. **(a)** Strategy for generating ALPK3 cardiac specific conditional knockout (cKO) mice. ALPK3 floxed mice (*f/f*) were crossed with *f/+; α MHC-Cre+* mice to generate cardiac specific ALPK3 knock out (*f/f; Cre+*, cKO) mice and control littermates (*ALPK3^{ff}*, Ctrl). **(b)** mRNA levels of ALPK3 in control (Ctrl, *n*=5) and cKO (*n*=3) mouse hearts. mRNA levels were normalized to *Gapdh*. **, *p* < 0.01 by Student's t-test. **(c)** Kaplan-Meier survival analysis of Ctrl and ALPK3 cKO mice. **(d)** H&E staining of Ctrl and ALPK3 cKO heart sections at postnatal day 2 (P2) and postnatal day 21 (P21). Scale bar, 1mm. **(e)-(g)** Echocardiography measurements of left ventricular internal diameter at **(e)** end-diastole (LVIDd), **(f)** end-systole (LVIDs), and **(g)** left ventricular (LV) systolic function (% of ejection fraction, ES) in Ctrl (blue, *n*=3-6) and cKO (red, *n*=3-8) mice at 2, 4, 6, and 8 weeks (w) after birth. NS, not statistically significant; *, *p* < 0.05; **, *p* < 0.01 by Student's t-test.

a**b****c****d****e****f****g**

Kinase activity was dispensable for the cardiac function of ALPK3

Since the kinase activity of other alpha protein kinases such as TRPM7 have been shown to possess physiological functions (Clark *et al.*, 2006), we next investigated whether the cardiac function of ALPK3 was dependent on its putative kinase activity. Within the alpha kinase domain of mouse ALPK3, the lysine residue at amino acid position 1420 (K1420) is conserved in all alpha kinases (Figure 3a) (Drennan and Ryazanov, 2004); it binds to the adenosine ring and the alpha phosphate of ATP and thus is essential for the kinase activity of alpha kinases (Drennan and Ryazanov, 2004). To investigate whether the loss of the putative kinase activity of ALPK3 would result in the DCM phenotypes observed in gKO and cKO mice, we next replaced ALPK3 lysine 1420 with arginine (K4120R) in mice using CRISPR-Cas9 genome editing technology (Figure 3b-c & Method—Mice) to ablate the potential kinase activity of ALPK3. Homozygous ALPK3 K1420R mice (Mut/Mut) did not exhibit premature lethality (data not shown). Echocardiographic measurements on Mut/Mut mice at 4-week and 8-week, two time points at which a trend of DCM phenotypes in cKO mice was observed, revealed comparable left ventricular size (Figure 3d-e) and cardiac contractile function (Figure 3f) as their control littermates. Hence, those data suggested that the kinase activity of ALPK3 was dispensable for its cardiac function, and ALPK3 likely behaved as a pseudokinase and functioned via interacting with other proteins (Boudeau *et al.*, 2006).

a

| | | | | | | |
|--------|--|-------------|--|---|---------------------|------|
| Q96QT4 | | TRPM7_HUMAN | | EFLSKEEMGG--GLRRAV-KVQCTWS-EHDILKSGHLYIIK | SFLPEVNTWSS----- | 1660 |
| Q923J1 | | TRPM7_MOUSE | | EFLSKEEMGG--GLRRAV-KVLCCTS-EHDILKSGHLYIIK | SFLPEVINTWSS----- | 1658 |
| Q9BX84 | | TRPM6_HUMAN | | QVLSREEMDG--GLRKAM-RVVSTWS-EDDILKPGQVFIVK | SFLPEVVRTWHK----- | 1816 |
| Q8CIR4 | | TRPM6_MOUSE | | QVLSQEEMDG--GLRKAM-RVISTWS-EDDVLKPGQVFIVK | SFLPEVVQTWYK----- | 1822 |
| Q96QP1 | | ALPK1_HUMAN | | KPSQLHRAHS--ALLLKYSKSELWTAQETIVYLG DYLTVK | KKGRQRNAPVWH--HLHQE | 1058 |
| Q9CXB8 | | ALPK1_MOUSE | | KSNQLQAHS--ALLLKYSKSELWTAQETVVYLG DYLVK | KKGRQRNAPVWH--YLHQE | 1044 |
| Q96L96 | | ALPK3_HUMAN | | VSEELRGGGYCGGLRKAS-QAKVIYG-LEPIFESGRTCIIK | -----VSSLLVFGP | 1656 |
| D3YUT2 | | ALPK3_MOUSE | | VSEELRGGGH--GLQKAS-RAKVIYG-LEPIFESGRTCIIK | -----VSSLLVFGP | 1429 |
| Q86TB3 | | ALPK2_HUMAN | | ATEELHFGEG--VHRKAF-RSTVMHG-LMPVFKPGHACVLK | -----VHNAIAYGT | 1964 |
| Q91ZB0 | | ALPK2_MOUSE | | STEELHFGEG--VHRKAF-RSKVMQG-LMPVFKPGHACVLK | -----VHNAVAHGT | 1937 |

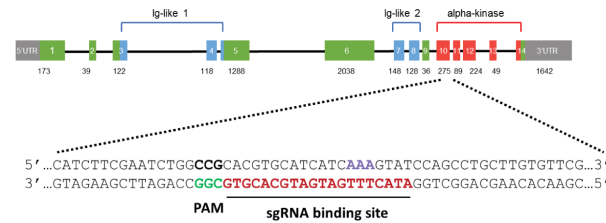
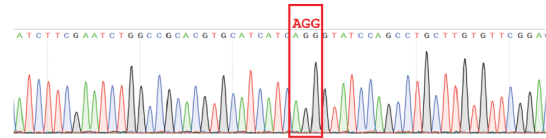
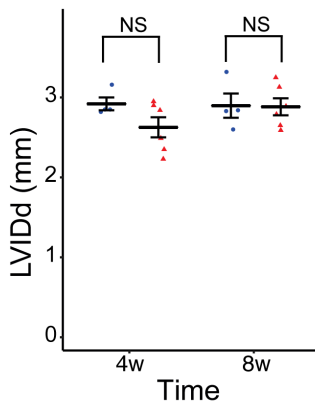
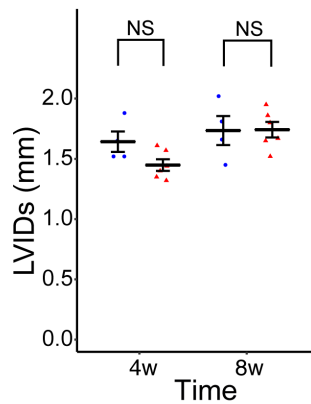
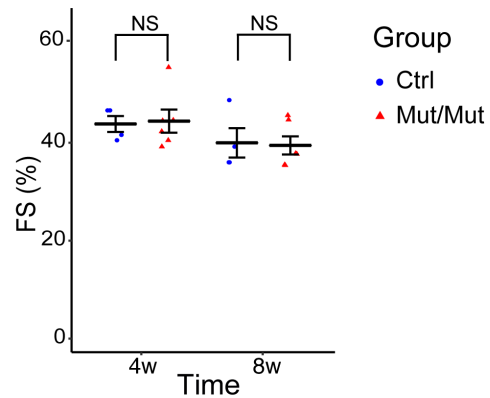
b**c****d****e****f**

Figure 3. Loss of ALPK3 kinase activity did not change cardiac function in mice. (a) Clustal Omega alignment of the alpha kinase domain of alpha kinases present in mouse and human. The invariant lysine residue was in red and highlighted. ALPK3 mouse sequence was boxed. **(b)** Strategy for generating ALPK3 K1420R knock-in mice by CRISPR-Cas9 genome editing system. **(c)** Validation of the AGG codon knock-in by sequencing. **(d)-(f)** Echocardiography measurements of left ventricular internal diameter at **(d)** end-diastole (LVIDd), **(e)** end-systole (LVIDs), and **(f)** left ventricular (LV) systolic function (% of fractional shortening, FS) in Ctrl (blue, n=4) and homozygous K1420R knock in (Mut/Mut) (red, n=6) mice at 4 and 8 weeks (w) after birth. NS, not statistically significant by Student's t-test.

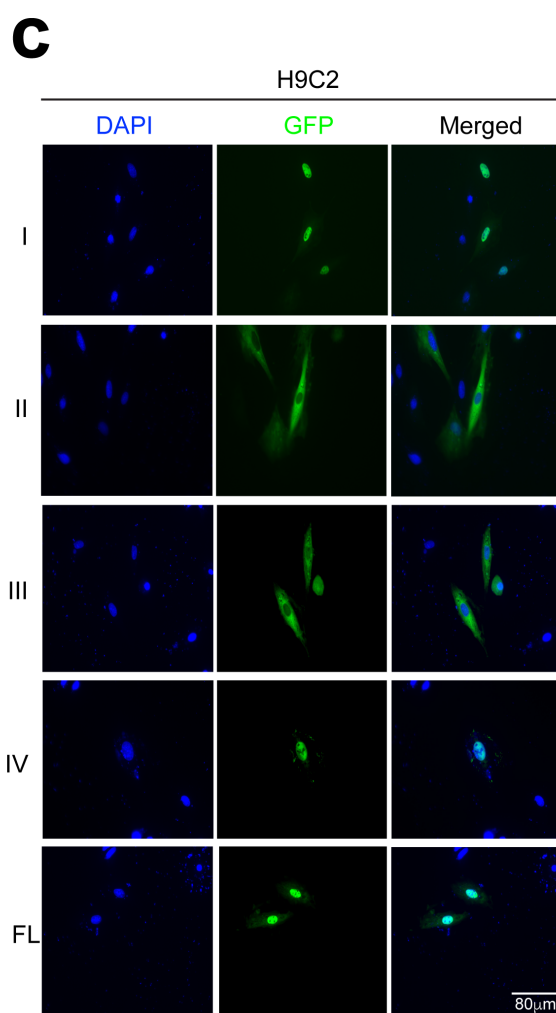
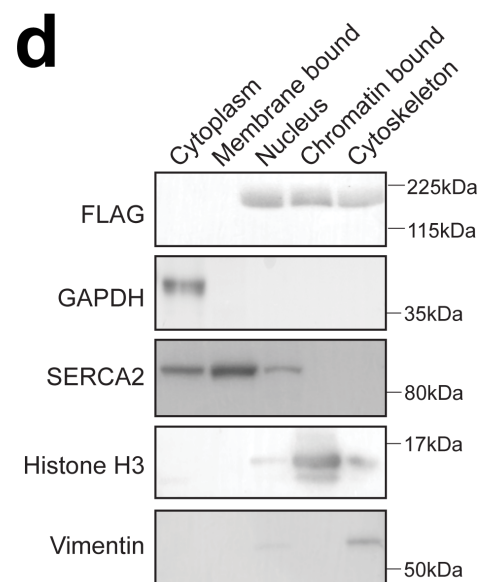
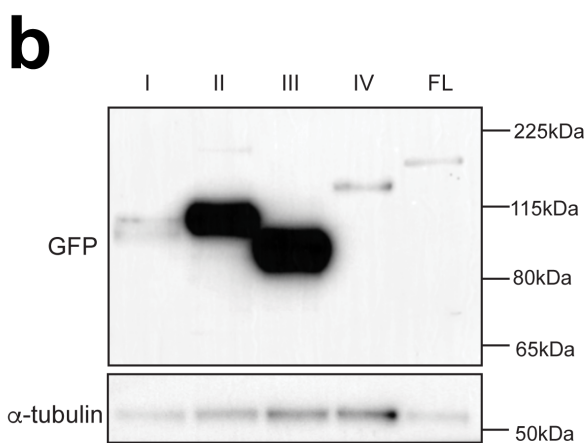
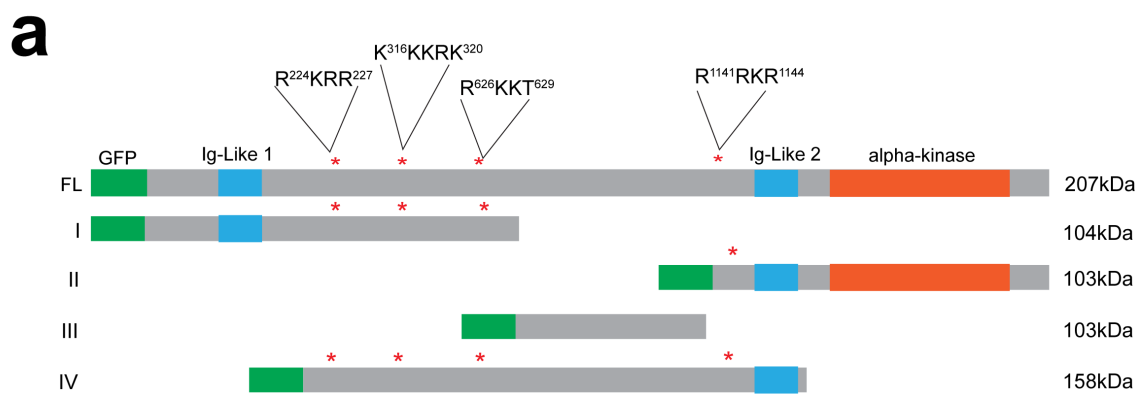
ALPK3 localized in the nucleus of cardiomyocyte

Since our data suggested that ALPK3 functioned via protein interactions, yet the localization of ALPK3 in cardiomyocyte was unknown, we next aimed to identify the subcellular localization at which those interactions might take place. *In silico* analysis predicted 4 nucleus localization signals (NLS's) in ALPK3, including R²²⁴KRR²²⁷, K³¹⁶KKRK³²⁰, R⁶²⁶KKT⁶²⁹, and R¹¹⁴¹RKR¹¹⁴⁴ (Figure 4a), suggesting that ALPK3 was a nucleus-localized protein. To identify the NLS's responsible for the nuclear localization of ALPK3, we constructed plasmids containing full length (FL) ALPK3 or truncated ALPK3 with different combinations of NLS's (constructs I-IV); each ALPK3 construct also contained a GFP sequence fused to its N terminal for visualization of the protein localization in cells (Figure 4a). The plasmids were successfully transfected into and expressed in rat cardiac myoblast H9C2 cells as examined by western blotting (Figure 4b). Fluorescent microscopic analysis on transfected H9C2 cells revealed that GFP signal was localized in the nucleus for H9C2 cells transfected with FL plasmid and plasmids I and IV, both of which contained R²²⁴KRR²²⁷, K³¹⁶KKRK³²⁰, and R⁶²⁶KKT⁶²⁹. In contrast, GFP signal was only observed in the cytoplasm of H9C2 cells transfected with plasmid II, which only contained R¹¹⁴¹RKR¹¹⁴⁴, and plasmid III, which did not contain any NLS's (Figure 4c). Taken together, those data suggested that ALPK3 was a nucleus-localized protein, and that NLS's R²²⁴KRR²²⁷, K³¹⁶KKRK³²⁰, and R⁶²⁶KKT⁶²⁹ in ALPK3 were responsible for its nuclear localization.

To detect the localization of ALPK3 *in vivo* without available ALPK3 antibodies, we knocked in a 3xFLAG cassette into the C terminal of the endogenous ALPK3 in mouse using CRISPR-Cas9 genome editing technology (Method—Mice). The knock-in was verified by PCR, DNA sequencing, and western blotting using a FLAG antibody; homozygous ALPK3-3xFLAG knock in mice also developed normally without observable cardiac defects, indicating that the knock in did not alter ALPK3 cardiac function (data not shown). We next performed a subcellular fractionation assay on whole heart lysate from ALPK3-3xFLAG homozygous knock in mice and

successfully isolated the proteins from the cytoplasm fraction, membrane bound fraction, nuclear fraction, chromatin bound fraction, and cytoskeletal fraction. Western blot analysis indicated that ALPK3-3xFLAG signal was highly enriched in the nuclear and chromatin bound fractions (Figure 4d), suggesting ALPK3 to be a nucleus-localized protein. Interestingly, an ALPK3-3xFLAG signal was also detected in the cytoskeleton fraction (Figure 4d). In an attempt to directly visualize ALPK3 localization in mouse cardiomyocyte, we performed an immunostaining using a FLAG antibody on ALPK3-3xFLAG cardiac tissue sections and isolated adult cardiomyocyte. Unfortunately, this approach yielded a low signal to noise ratio under a fluorescent microscope (data not shown). Nonetheless, our transfection data and subcellular fractionation data provided convincing evidence for the nucleus-localization of ALPK3 in cardiomyocyte.

Figure 4. ALPK3 localized in the nucleus of cardiomyocyte. (a) *In silico* prediction of the nucleus localization signals (NLS's) in ALPK3. Functional domains including Ig-like 1 (blue), Ig-like 2 (blue) and alpha kinase domain (orange) in ALPK3 and GFP (green) were labeled. NLS's were marked by * with their sequences and amino acid numbers indicated. Full length (FL) and truncated GFP-ALPK3 (I to IV) constructs were labeled, with their corresponding protein molecular weight (kDa) marked on the right. (b) Confirmation of the expression of FL and truncated GFP-ALPK3 proteins in H9C2 cells after transfection. α -tubulin was used as a loading control. (c) Immunofluorescent microscopic analysis of H9C2 cells transfected with full length or truncated GFP-ALPK3 plasmids. Individual channels of DNA stain DAPI (blue) and GFP (green) as well as merged-channel images were shown. Scale bar, 80 μ m. (d) Western blot analysis of whole heart tissue fractionations in ALPK3-3xFLAG homozygous knock in mice. Tissue fractions (cytoplasm, membrane bound, nucleus, chromatin bound, cytoskeleton) and their corresponding markers (GAPDH, SERCA2, Histone H3, Histone H3, Vimentin) were shown.



Identification of potential ALPK3 interacting proteins

To detect the potential proteins interacting with ALPK3, we performed a FLAG co-immunoprecipitation (co-IP) on cardiac tissue lysates from 2 homozygous ALPK3-3xFLAG mice and 2 control littermates. Mass spectrometry on the FLAG co-IP pulled down proteins identified 233 unique peptides, with ALPK3 exclusively present in the pulled down samples from homozygous ALPK3-3xFLAG hearts. After performing statistical filtering of the mass spectrometry data (Method—Mass spectrometry and statistical filtering), we identified 38 unique proteins potentially interacting with ALPK3 (Table 1). Gene Ontology (GO) analysis on the 38 proteins revealed that those proteins were enriched in the biological processes of muscle structure development (GO:0061061, 8 proteins), muscle cell differentiation (GO:0042692, 6 proteins), muscle contraction (GO:0006936, 5 proteins), and energy derivation by oxidation of organic compounds (GO:0015980, 5 proteins) (Figure 5), suggesting that ALPK3 interacted with proteins essential for cardiac muscle development, function, and metabolism.

Table 1. List of proteins enriched in FLAG-IP mass spectrometry samples. Enrichment was calculated by dividing the Intensity of a peptide in homozygous ALPK3-3xFLAG knock in mouse hearts by the intensity of the same peptide in control mouse hearts. Inf, infinity. Proteins were sorted by enrichment in descending order.

| Number | Protein | Enrichment |
|---------------|----------------|-------------------|
| 1 | Rpl27a | Inf |
| 2 | Hmgb2 | Inf |
| 3 | Tmod1 | Inf |
| 4 | Sec31b | Inf |
| 5 | Alpk3 | Inf |
| 6 | Pygm | Inf |
| 7 | Suclg1 | Inf |
| 8 | Myh9 | 58.02 |
| 9 | Des | 47.72 |
| 10 | Actn2 | 35.21 |
| 11 | Capza2 | 7.28 |
| 12 | Myh4;Myh1 | 5.96 |
| 13 | Nhlrc1 | 5.94 |
| 14 | Tufm | 5.88 |
| 15 | Tf | 5.38 |
| 16 | Myh6;Myh7 | 5.04 |
| 17 | Myl3 | 4.91 |
| 18 | Atp2a2 | 4.76 |
| 19 | Fga | 4.76 |
| 20 | Myl6;Myl6b | 3.88 |
| 21 | Mdh2 | 3.76 |
| 22 | Acadvl | 3.68 |
| 23 | Gsn | 3.57 |
| 24 | Fkbp3 | 3.53 |
| 25 | Ddx3x | 3.31 |
| 26 | Stk38l | 3.24 |
| 27 | Hspa8 | 3.21 |
| 28 | Ak1 | 3.06 |
| 29 | Epm2a | 2.94 |
| 30 | Aco2 | 2.67 |
| 31 | Tmod3 | 2.42 |
| 32 | Stk38 | 2.40 |
| 33 | Ndufa4 | 2.37 |
| 34 | Slc25a3 | 2.32 |
| 35 | Rpl23a | 2.30 |
| 36 | Csrp3 | 2.20 |
| 37 | Znf706 | 2.04 |
| 38 | Hist1h1e | 2.01 |

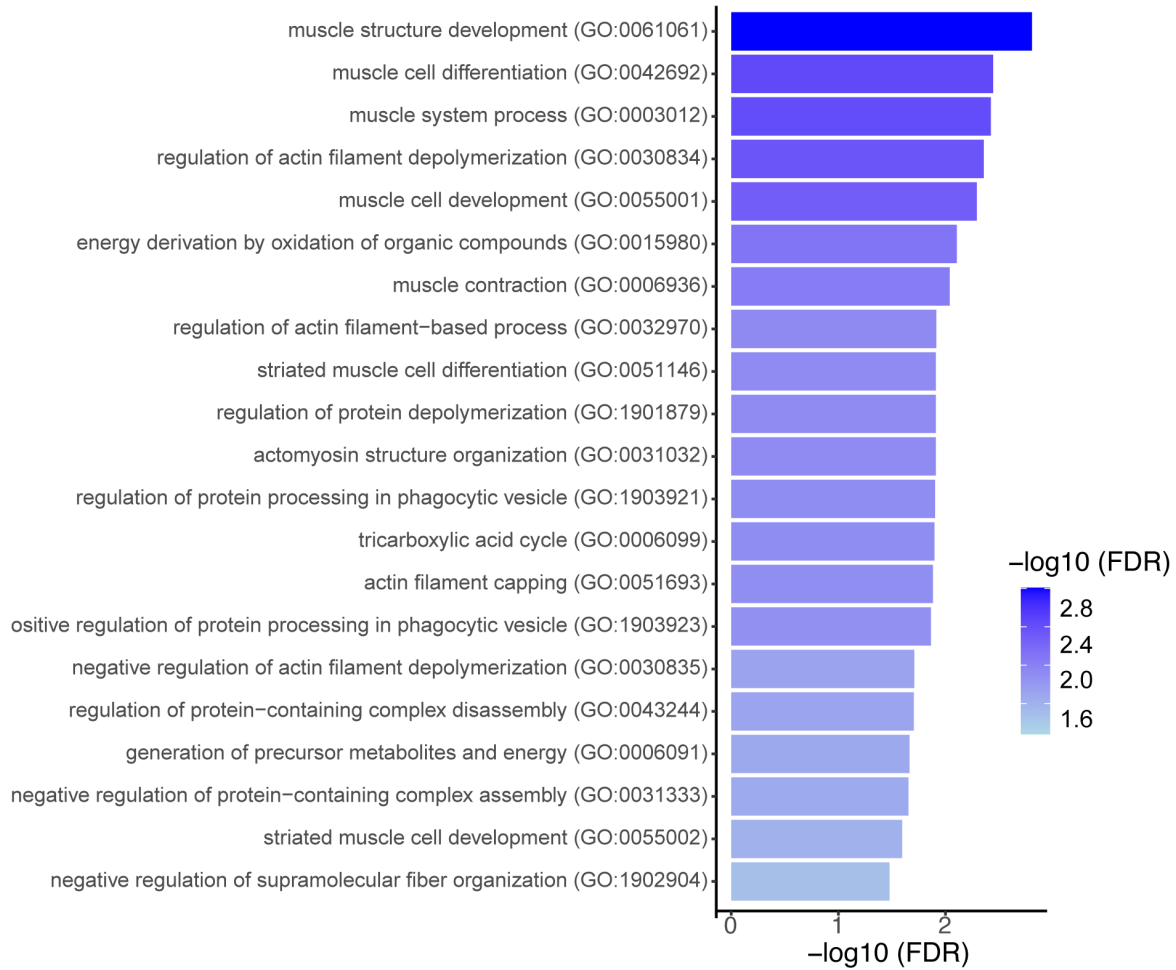


Figure 5. ALPK3 interacted with proteins essential for cardiac development and function. Gene Ontology (GO) analysis of FLAG-IP enriched proteins in Table 1. GO biological function terms and their respective significance ($-\log_{10}$ of false discovery rate (FDR)) were shown.

DISCUSSION

ALPK3 is one of the six alpha kinases identified in human (Middelbeek *et al.*, 2010), and its enriched expressions in heart and skeletal muscles (Fagerberg *et al.*, 2014) suggest for its tissue specific function. Recently, clinical studies have revealed that the biallelic truncating mutations in ALPK3 are associated with pediatric cardiomyopathy (Çağlayan *et al.*, 2017; Herkert *et al.*, 2020; Jaouadi *et al.*, 2018; Phelan *et al.*, 2016), further implicating the cardiac specific function of ALPK3. Using ALPK3 global knockout and cardiac specific knockout mouse models, our data showed that ALPK3 was indispensable for cardiac function and development, and that the global and cardiac specific loss of ALPK3 led to dilated cardiomyopathy and premature lethality in mice (Figure 1&2). Intriguingly, by mutating the invariant lysine residue 1420 to arginine in the alpha kinase domain of ALPK3 in mice, our data further suggested that the putative kinase activity of ALPK3 was dispensable for its cardiac function, as homozygous K1420R mutation knock in mice develop normally without observable cardiac defects (Figure 3d-f). Hence, under normal physiological condition, ALPK3 likely exerts its cardiac function independently of its putative kinase activity, possibly via protein interactions similar to other pseudokinases.

ALPK3 has been suggested to localize in cell nucleus (Hosoda *et al.*, 2001), yet its exact subcellular localization in cardiomyocyte was elusive. Using *in silico* analysis, we predicted 4 potential nucleus localization signals (NLS's) in ALPK3 (Figure 4a). By transfecting full length and truncated ALPK3 plasmids containing different combinations of the 4 NLS's into H9C2 cells, our data corroborated for the nuclear localization of ALPK3 in cardiomyocyte, and we further identified NLS's R²²⁴KRR²²⁷, K³¹⁶KKRK³²⁰, and R⁶²⁶KKT⁶²⁹ in ALPK3 to be responsible for its nucleus-localization (Figure 4c). Additionally, our subcellular fractionation assay on ALPK3-3xFLAG tagged mice showed that ALPK3 was highly enriched in the nucleus fraction (Figure 4d). Unfortunately, while we attempted to perform immunostaining using a FLAG antibody on ALPK3-3xFLAG tagged mouse cardiomyocytes for the direct observation of ALPK3 subcellular

localization in cardiomyocyte, our FLAG antibody yielded a low signal to noise ratio in fluorescent microscopy (data not shown). One possibility is that while the FLAG antibody is able to detect its ALPK3 epitope in the denaturalized peptide in western blot, the access to the epitope is obstructed in the native conformation of the ALPK3-3xFLAG protein. Alternatively, it is possible that the expression level of ALPK3 falls below the limit for detecting a positive fluorescent signal, making the direct observation of ALPK3 localization in mouse cardiomyocytes challenging. Nonetheless, our *in silico* prediction, transfection data, and subcellular fractionation data strongly suggest that ALPK3 localizes in the nucleus of cardiomyocyte. Since the kinase activity is dispensable for the cardiac function of ALPK3, the nuclear localization of ALPK3 suggests that ALPK3 functions via interacting with other protein factors in the nucleus and in turn regulates the gene expressions essential for cardiac development and function.

To identify the potential protein interactors of ALPK3, we performed a co-immunoprecipitation assay on the whole heart lysate from ALPK3-3xFLAG mice and identified the pulled-down proteins by mass spectrometry. The highly enriched proteins in the pulled-down fraction were involved in pathways of muscle cell differentiation, muscle structure development, and muscle function (Figure 5), suggesting that ALPK3 interacted with proteins essential for cardiac muscle function and development. While both our *in vitro* transfection data and subcellular fractionation data suggest that ALPK3 is a nucleus localized protein, interestingly, only a few of those pulled-down proteins (e.g., HMGB2, DDX3X, HIST1H1E) are localized in the nucleus; the majority of the other proteins are muscle specific structural proteins such as TMOD1, MYH9, MYH6, and MYH7. Two explanations are possible regarding the discrepancies between our co-IP data and localization data. First, in addition to the nucleus, ALPK3 might also co-localize with cardiac muscle structural proteins. In support of this possibility, we detected an ALPK3-3xFLAG signal in the cytoskeleton fraction in our subcellular fractionation assay (Figure 4d). However, the methodology of the fractionation assay, in which the cytoskeletal fraction

proteins were lysed from the pellet remained after the extraction of all other fractions, might introduce contaminants in this fraction. Hence, protocols specifically designed for cytoskeletal protein extraction are required to verify whether ALPK3 might indeed also co-localize with cytoskeleton. Second, the co-IP approach might not be able to detect the protein interactions of ALPK3 under native physiological condition with high sensitivity. Due to the nuclear localization of ALPK3, RIPA buffer, which contains sodium dodecyl sulfate, was necessary to disrupt the nuclear membrane and to lyse the tissue for ALPK3 protein. The presence of a strong detergent leads to the possibility of disrupting protein-protein interactions (PPIs), especially the ones that are weak or transient (Gingras *et al.*, 2019). Hence, while ALPK3 might still interact with nuclear proteins, those interactions are not able to be captured by the biochemical approach of co-IP.

To bypass the limitation of co-IP in identifying PPIs with ALPK3, an alternative approach by proximity biotinylation can be utilized (Gingras *et al.*, 2019). By inserting a biotin ligase to the N or C terminal of a protein of interest, the fusion protein can serve as a bait to promiscuously biotinylate the proteins in its close proximity; the biotinylated proteins can then be affinity-captured by streptavidin and identified by mass spectrometry (Roux *et al.*, 2012). This approach allows for the *in vivo* labeling of proteins in close proximity (about 10nm) of the bait, which can then be statistically filtered for potential protein interactors of the bait (Gingras *et al.*, 2019). Recently, we have knocked in a BioID2 cassette into the cardiac dyad protein JPH2 and used proximity biotinylation to identify cardiac dyad proteome (Feng *et al.*, 2020), providing a proof of concept for using this approach to identify PPIs in the hearts of live mice. To bypass the limitation of co-IP, we have knocked in a BioID2 cassette to the C terminal of the endogenous ALPK3 protein in mice. Once the knock in of BioID2 is verified, *in vivo* biotinylation followed by streptavidin pull-down and mass spectrometry for peptide identification will be used to identify the proteins in proximity of ALPK3-BioID2 fusion protein. Potential PPIs will be analyzed by computational programs such as Significance Analysis of INTeractome (SAINT) (Choi *et al.*, 2012) and CompPASS (Sowa *et al.*, 2009), and high-confidence interacting proteins from the

proximity biotinylation approach will be compared with the co-IP data to identify the proteins most likely to interact with ALPK3. Those potential ALPK3-interacting proteins will then be analyzed by Gene Ontology of cellular components and biological functions to reveal whether they are nucleus-localized proteins regulating gene expression.

To note, the protein structure of ALPK3 hints at its unique mechanism of protein interaction. ALPK3 contains one Ig-like domain at its N terminal, one Ig-like domain at its C terminal, and an alpha protein kinase domain at its C terminal (Middelbeek *et al.*, 2010). The long region between the two Ig like domains does not contain any known secondary structures and is predicted to be disordered (Supplemental Figure 1). Biophysically, intrinsically disordered regions (IDRs) were shown to undergo phase separation via multivalent interaction, leading to the formation of biomolecular condensates (Banani *et al.*, 2017). Biomolecular condensates have been proposed as models for transcriptional regulation (Daneshvar *et al.*, 2020; Sabari *et al.*, 2018) in the nucleus of human and mouse embryonic stem cells as well as oncogenic signaling in cytoplasm of cancer cells (Tulpule *et al.*, 2021; Zhang *et al.*, 2020). One way by which biomolecular condensates function is to accelerate reaction rates by concentrating molecules, similar to scaffold proteins (Banani *et al.*, 2017). Interestingly, pseudokinases, while lacking catalytic activities, can serve as scaffold proteins and facilitate the biological functions of their interactors (Mace and Murphy, 2021). Hence, it is possible that while the putative kinase activity of ALPK3 is dispensable for its cardiac function, ALPK3 might promote the formation of biomolecular condensates via its IDRs, and those condensates in turn serve as hubs for biological processes necessary for cardiac function to occur. Considering for the nuclear localization of ALPK3, those condensates might recruit protein factors for gene regulation (Sabari *et al.*, 2018). By performing a streptavidin immunostaining on isolated cardiomyocyte from biotin-treated ALPK3-BiOID2 knock in mice, we will be able to test whether ALPK3 along with the proteins in its proximity indeed form distinct puncta structures in cell nucleus, a preliminary evidence for the ability of ALPK3 to form biomolecular condensates (Patel *et al.*,

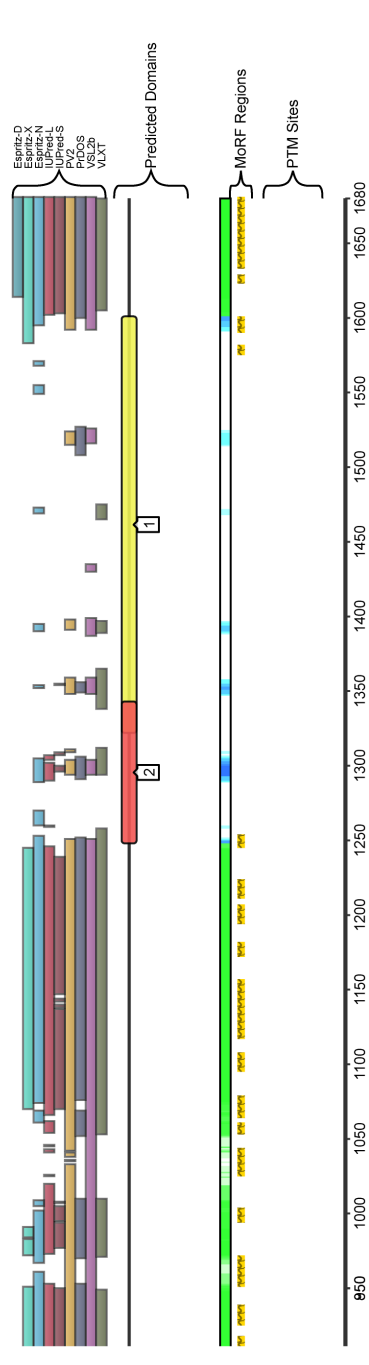
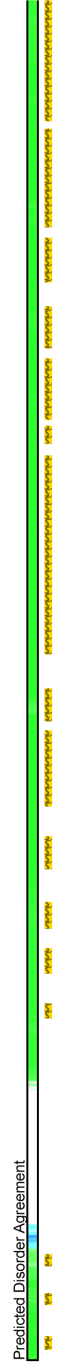
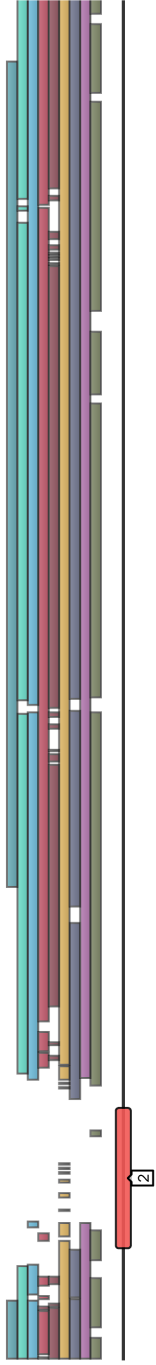
2015). Furthermore, a previous study has utilized proximity biotinylation to identify proteins in biomolecular condensates (Yu *et al.*, 2021). Hence, if ALPK3 does undergo biomolecular condensate formation *in vivo*, we anticipate that our proximity biotinylation approach proposed above will be able to capture the protein factors within the condensates. Those protein factors could be further analyzed to determine whether they play a role in gene regulation, contributing to the mechanistic basis of ALPK3 cardiac function.

APPENDIX

Appendix 1: Supplemental Figure 1

Supplemental Figure 1. ALPK3 contains intrinsically disordered regions (IDRs). IDRs were predicted by Database of Disordered Protein Predictions (D2P2). Algorithms used to predict IDRs were listed under “Disorder”, with their corresponding results colored in the schematic diagram. The amino acid locations as well as the Ig-like domains (red) and alpha kinase domain (yellow) of ALPK3 were shown for reference.

ENSMUSP00000102971



- Key:**
- Predicted SCOP Structure
 - Weaker Support
 - Predicted Disorder
 - Predicted MoRFs
 - Curated PTM Site
- Disorder:**
- Espritz-D
 - Espritz-X
 - Espritz-N
 - IUPred-L
 - IUPred-S
 - PV2
 - PIDOS
 - VSL2b
 - VLXT
- Superfamilies:**
- [1] Protein kinase-like (PK-like)
 - [2] Immunoglobulin

REFERENCES

- Agah, R., Frenkel, P.A., French, B.A., Michael, L.H., Overbeek, P.A., and Schneider, M.D. (1997). Gene recombination in postmitotic cells. Targeted expression of Cre recombinase provokes cardiac-restricted, site-specific rearrangement in adult ventricular muscle in vivo. *J. Clin. Invest.* *100*, 169–179.
- Almomani, R., Verhagen, J.M.A., Herkert, J.C., Brosens, E., van Spaendonck-Zwarts, K.Y., Asimaki, A., van der Zwaag, P.A., Frohn-Mulder, I.M.E., Bertoli-Avella, A.M., Boven, L.G., van Slegtenhorst, M.A., van der Smagt, J.J., van IJcken, W.F.J., Timmer, B., van Stuijvenberg, M., Verdijk, R.M., Saffitz, J.E., du Plessis, F.A., Michels, M., Hofstra, R.M.W., Sinke, R.J., van Tintelen, J.P., Wessels, M.W., Jongbloed, J.D.H., and van de Laar, I.M.B.H. (2016). Biallelic Truncating Mutations in ALPK3 Cause Severe Pediatric Cardiomyopathy. *Journal of the American College of Cardiology* *67*, 515–525.
- Banani, S.F., Lee, H.O., Hyman, A.A., and Rosen, M.K. (2017). Biomolecular condensates: organizers of cellular biochemistry. *Nat Rev Mol Cell Biol* *18*, 285–298.
- Bircan, H.A., Gurbuz, N., Pataer, A., Caner, A., Kahraman, N., Bayraktar, E., Bayraktar, R., Erdogan, M.A., Kabil, N., and Ozpolat, B. (2018). Elongation factor-2 kinase (eEF-2K) expression is associated with poor patient survival and promotes proliferation, invasion and tumor growth of lung cancer. *Lung Cancer* *124*, 31–39.
- Bogomolovas, J., Feng, W., Yu, M.D., Huang, S., Zhang, L., Trexler, C., Gu, Y., Spinozzi, S., and Chen, J. (2020). Atypical ALPK2 kinase is not essential for cardiac development and function. *American Journal of Physiology-Heart and Circulatory Physiology* *318*, H1509–H1515.
- Boudeau, J., Miranda-Saavedra, D., Barton, G.J., and Alessi, D.R. (2006). Emerging roles of pseudokinases. *Trends in Cell Biology* *16*, 443–452.
- Braunwald, E., and Marian, A.J. (2017). Pediatric Cardiomyopathies. 855–893.
- Brieler, J., Breeden, M.A., Tucker, J., University, S.L., and Louis, S. (2017). Cardiomyopathy: An Overview. *96*, 8.
- Çağlayan, A.O., Sezer, R.G., Kaymakçalan, H., Ulgen, E., Yavuz, T., Baranoski, J.F., Bozaykut, A., Harmanci, A.S., Yalcin, Y., Youngblood, M.W., Yasuno, K., Bilgüvar, K., and Gunel, M. (2017). ALPK3 gene mutation in a patient with congenital cardiomyopathy and dysmorphic features. *Cold Spring Harb Mol Case Stud* *3*, a001859.
- Choi, H., Liu, G., Mellacheruvu, D., Tyers, M., Gingras, A., and Nesvizhskii, A.I. (2012). Analyzing Protein-Protein Interactions from Affinity Purification-Mass Spectrometry Data with SAINT. *Current Protocols in Bioinformatics* *39*.
- Clark, K., Langeslag, M., van Leeuwen, B., Ran, L., Ryazanov, A.G., Figdor, C.G., Moolenaar, W.H., Jalink, K., and van Leeuwen, F.N. (2006). TRPM7, a novel regulator of actomyosin contractility and cell adhesion. *EMBO J* *25*, 290–301.
- Daneshvar, K., Ardehali, M.B., Klein, I.A., Hsieh, F.-K., Kratkiewicz, A.J., Mahpour, A., Cancelliere, S.O.L., Zhou, C., Cook, B.M., Li, W., Pondick, J.V., Gupta, S.K., Moran, S.P., Young, R.A., Kingston, R.E., and Mullen, A.C. (2020). lncRNA DIGIT and BRD3 protein form

phase-separated condensates to regulate endoderm differentiation. *Nat Cell Biol* 22, 1211–1222.

Drennan, D., and Ryazanov, A.G. (2004). Alpha-kinases: analysis of the family and comparison with conventional protein kinases. *Progress in Biophysics and Molecular Biology* 85, 1–32.

Fagerberg, L., Hallström, B.M., Oksvold, P., Kampf, C., Djureinovic, D., Odeberg, J., Habuka, M., Tahmasebpoor, S., Danielsson, A., Edlund, K., Asplund, A., Sjöstedt, E., Lundberg, E., Szigartyo, C.A.-K., Skogs, M., Takanen, J.O., Berling, H., Tegel, H., Mulder, J., Nilsson, P., Schwenk, J.M., Lindskog, C., Danielsson, F., Mardinoglu, A., Sivertsson, Å., von Feilitzen, K., Forsberg, M., Zwahlen, M., Olsson, I., Navani, S., Huss, M., Nielsen, J., Ponten, F., and Uhlén, M. (2014). Analysis of the Human Tissue-specific Expression by Genome-wide Integration of Transcriptomics and Antibody-based Proteomics. *Molecular & Cellular Proteomics* 13, 397–406.

Fang, X., Bogomolovas, J., Wu, T., Zhang, W., Liu, C., Veevers, J., Stroud, M.J., Zhang, Z., Ma, X., Mu, Y., Lao, D.-H., Dalton, N.D., Gu, Y., Wang, C., Wang, M., Liang, Y., Lange, S., Ouyang, K., Peterson, K.L., Evans, S.M., and Chen, J. (2017). Loss-of-function mutations in co-chaperone BAG3 destabilize small HSPs and cause cardiomyopathy. *Journal of Clinical Investigation* 127, 3189–3200.

Feng, W., Liu, C., Spinozzi, S., Wang, L., Evans, S.M., and Chen, J. (2020). Identifying the Cardiac Dyad Proteome In Vivo by a BioID2 Knock-In Strategy. *Circulation* 141, 940–942.

Gingras, A.-C., Abe, K.T., and Raught, B. (2019). Getting to know the neighborhood: using proximity-dependent biotinylation to characterize protein complexes and map organelles. *Current Opinion in Chemical Biology* 48, 44–54.

Gluzman, Y. (1981). SV40-transformed simian cells support the replication of early SV40 mutants. *Cell* 23, 175–182.

Goldman, L., and Schafer, A.I. (2015). *Goldman-Cecil Medicine : Expert Consult - Online* (Saint Louis, UNITED STATES: Elsevier).

Hayashi, S., Lewis, P., Pevny, L., and McMahon, A.P. (2002). Efficient gene modulation in mouse epiblast using a Sox2Cre transgenic mouse strain. *Mechanisms of Development* 119, S97–S101.

Herkert, J.C., Verhagen, J.M.A., Yotti, R., Haghghi, A., Phelan, D.G., James, P.A., Brown, N.J., Stutterd, C., Macciocca, I., Leong, K., Bulthuis, M.L.C., van Bever, Y., van Slegtenhorst, M.A., Boven, L.G., Roberts, A.E., Agarwal, R., Seidman, J., Lakdawala, N.K., Fernández-Avilés, F., Burke, M.A., Pierpont, M.Ella., Braunlin, E., Çağlayan, A.O., Barge-Schaapveld, D.Q.C.M., Birnie, E., van Osch-Gevers, L., van Langen, I.M., Jongbloed, J.D.H., Lockhart, P.J., Amor, D.J., Seidman, C.E., and van de Laar, I.M.B.H. (2020). Expanding the clinical and genetic spectrum of ALPK3 variants: Phenotypes identified in pediatric cardiomyopathy patients and adults with heterozygous variants. *American Heart Journal* 225, 108–119.

Horman, S., Browne, G.J., Krause, U., Patel, J.V., Vertommen, D., Bertrand, L., Lavoigne, A., Hue, L., Proud, C.G., and Rider, M.H. (2002). Activation of AMP-Activated Protein Kinase Leads to the Phosphorylation of Elongation Factor 2 and an Inhibition of Protein Synthesis. *Current Biology* 12, 1419–1423.

- Hosoda, T., Monzen, K., Hiroi, Y., Oka, T., Takimoto, E., Yazaki, Y., Nagai, R., and Komuro, I. (2001). A Novel Myocyte-specific Gene Midori Promotes the Differentiation of P19CL6 Cells into Cardiomyocytes. *Journal of Biological Chemistry* 276, 35978–35989.
- Jaouadi, H., Kraoua, L., Chaker, L., Atkinson, A., Delague, V., Levy, N., Benkhalifa, R., Mrad, R., Abdelhak, S., and Zaffran, S. (2018). Novel ALPK3 mutation in a Tunisian patient with pediatric cardiomyopathy and facio-thoraco-skeletal features. *J Hum Genet* 63, 1077–1082.
- Kochanek, K.D., Xu, J., and Arias, E. (2020). Mortality in the United States, 2019. NCHS Data Brief 8.
- Liu, C., Spinozzi, S., Chen, J.-Y., Fang, X., Feng, W., Perkins, G., Cattaneo, P., Guimarães-Camboa, N., Dalton, N.D., Peterson, K.L., Wu, T., Ouyang, K., Fu, X.-D., Evans, S.M., and Chen, J. (2019). Nexilin Is a New Component of Junctional Membrane Complexes Required for Cardiac T-Tubule Formation. *Circulation* 140, 55–66.
- Mace, P.D., and Murphy, J.M. (2021). There's more to death than life: non-catalytic functions in kinase and pseudokinase signaling. *Journal of Biological Chemistry* 100705.
- Maron, B.J., Towbin, J.A., Thiene, G., Antzelevitch, C., Corrado, D., Arnett, D., Moss, A.J., Seidman, C.E., and Young, J.B. (2006). Contemporary Definitions and Classification of the Cardiomyopathies: An American Heart Association Scientific Statement From the Council on Clinical Cardiology, Heart Failure and Transplantation Committee; Quality of Care and Outcomes Research and Functional Genomics and Translational Biology Interdisciplinary Working Groups; and Council on Epidemiology and Prevention. *Circulation* 113, 1807–1816.
- Middelbeek, J., Clark, K., Venselaar, H., Huynen, M.A., and van Leeuwen, F.N. (2010). The alpha-kinase family: an exceptional branch on the protein kinase tree. *Cell. Mol. Life Sci.* 67, 875–890.
- Mu, Y., Yu, H., Wu, T., Zhang, J., Evans, S.M., and Chen, J. (2020). O-linked β -N-acetylglucosamine transferase plays an essential role in heart development through regulating angiotensin-1. *PLoS Genet* 16, e1008730.
- Patel, A., Lee, H.O., Jawerth, L., Maharana, S., Jahnel, M., Hein, M.Y., Stoyanov, S., Mahamid, J., Saha, S., Franzmann, T.M., Pozniakovski, A., Poser, I., Maghelli, N., Royer, L.A., Weigert, M., Myers, E.W., Grill, S., Drechsel, D., Hyman, A.A., and Alberti, S. (2015). A Liquid-to-Solid Phase Transition of the ALS Protein FUS Accelerated by Disease Mutation. *Cell* 162, 1066–1077.
- Phelan, D.G., Anderson, D.J., Howden, S.E., Wong, R.C.B., Hickey, P.F., Pope, K., Wilson, G.R., Pébay, A., Davis, A.M., Petrou, S., Elefanty, A.G., Stanley, E.G., James, P.A., Macciocca, I., Bahlo, M., Cheung, M.M., Amor, D.J., Elliott, D.A., and Lockhart, P.J. (2016). ALPK3-deficient cardiomyocytes generated from patient-derived induced pluripotent stem cells and mutant human embryonic stem cells display abnormal calcium handling and establish that ALPK3 deficiency underlies familial cardiomyopathy. *Eur Heart J* 37, 2586–2590.
- Rodríguez, C.I., Buchholz, F., Galloway, J., Sequerra, R., Kasper, J., Ayala, R., Stewart, A.F., and Dymecki, S.M. (2000). High-efficiency deleter mice show that FLPe is an alternative to Cre-loxP. *Nat Genet* 25, 139–140.

Roux, K.J., Kim, D.I., Raida, M., and Burke, B. (2012). A promiscuous biotin ligase fusion protein identifies proximal and interacting proteins in mammalian cells. *Journal of Cell Biology* 196, 801–810.

Sabari, B.R., Dall’Agnese, A., Boija, A., Klein, I.A., Coffey, E.L., Shrinivas, K., Abraham, B.J., Hannett, N.M., Zamudio, A.V., Manteiga, J.C., Li, C.H., Guo, Y.E., Day, D.S., Schuijers, J., Vasile, E., Malik, S., Hnisz, D., Lee, T.I., Cisse, I.I., Roeder, R.G., Sharp, P.A., Chakraborty, A.K., and Young, R.A. (2018). Coactivator condensation at super-enhancers links phase separation and gene control. *Science* 361, eaar3958.

Scheeff, Eric D., and Bourne, Philip E (2005). Structural Evolution of the Protein Kinase–Like Superfamily. *PLOS COMPUTATIONAL BIOLOGY* 1, 0356–0381.

Schlingmann, K.P., Waldegger, S., Konrad, M., Chubanov, V., and Gudermann, T. (2007). TRPM6 and TRPM7—Gatekeepers of human magnesium metabolism. *Biochimica et Biophysica Acta (BBA) - Molecular Basis of Disease* 1772, 813–821.

Shao, C.Y., Crary, J.F., Rao, C., Sacktor, T.C., and Mirra, S.S. (2006). Atypical Protein Kinase C in Neurodegenerative Disease II: PKC δ /L in Tauopathies and α -Synucleinopathies. *J Neuropathol Exp Neurol* 65, 9.

Sowa, M.E., Bennett, E.J., Gygi, S.P., and Harper, J.W. (2009). Defining the Human Deubiquitinating Enzyme Interaction Landscape. *Cell* 138, 389–403.

Tulpule, A., Guan, J., Neel, D.S., Allegakoen, H.R., Lin, Y.P., Brown, D., Chou, Y.-T., Heslin, A., Chatterjee, N., Perati, S., Menon, S., Nguyen, T.A., Debnath, J., Ramirez, A.D., Shi, X., Yang, B., Feng, S., Makhija, S., Huang, B., and Bivona, T.G. (2021). Kinase-mediated RAS signaling via membraneless cytoplasmic protein granules. *Cell* S0092867421003627.

Virani, S.S., Alonso, A., Aparicio, H.J., Benjamin, E.J., Bittencourt, M.S., Callaway, C.W., Carson, A.P., Chamberlain, A.M., Cheng, S., Delling, F.N., Elkind, M.S.V., Evenson, K.R., Ferguson, J.F., Gupta, D.K., Khan, S.S., Kissela, B.M., Knutson, K.L., Lee, C.D., Lewis, T.T., Liu, J., Loop, M.S., Lutsey, P.L., Ma, J., Mackey, J., Martin, S.S., Matchar, D.B., Mussolino, M.E., Navaneethan, S.D., Perak, A.M., Roth, G.A., Samad, Z., Satou, G.M., Schroeder, E.B., Shah, S.H., Shay, C.M., Stokes, A., VanWagner, L.B., Wang, N.-Y., Tsao, C.W., and On behalf of the American Heart Association Council on Epidemiology and Prevention Statistics Committee and Stroke Statistics Subcommittee (2021). Heart Disease and Stroke Statistics—2021 Update: A Report From the American Heart Association. *Circulation* 143.

Wu, T., Mu, Y., Bogomolovas, J., Fang, X., Veevers, J., Nowak, R.B., Pappas, C.T., Gregorio, C.C., Evans, S.M., Fowler, V.M., and Chen, J. (2017). HSPB7 is indispensable for heart development by modulating actin filament assembly. *Proc Natl Acad Sci USA* 114, 11956–11961.

Yu, H., Lu, S., Gasior, K., Singh, D., Vazquez-Sanchez, S., Tapia, O., Toprani, D., Beccari, M.S., Yates, J.R., Da Cruz, S., Newby, J.M., Lafarga, M., Gladfelter, A.S., Villa, E., and Cleveland, D.W. (2021). HSP70 chaperones RNA-free TDP-43 into anisotropic intranuclear liquid spherical shells. *Science* 371, eabb4309.

Zhang, J.Z., Lu, T.-W., Stolerman, L.M., Tenner, B., Yang, J.R., Zhang, J.-F., Falcke, M., Rangamani, P., Taylor, S.S., Mehta, S., and Zhang, J. (2020). Phase Separation of a PKA

Regulatory Subunit Controls cAMP Compartmentation and Oncogenic Signaling. *Cell* 182, 1531-1544.e15.

Zhou, P., She, Y., Dong, N., Li, P., He, H., Borio, A., Wu, Q., Lu, S., Ding, X., Cao, Y., Xu, Y., Gao, W., Dong, M., Ding, J., Wang, D.-C., Zamyatina, A., and Shao, F. (2018). Alpha-kinase 1 is a cytosolic innate immune receptor for bacterial ADP-heptose. *Nature* 561, 122–126.